

Matched Pressure Properties of Low Altitude Plumes

Peter C. Sukanek*

*Air Force Rocket Propulsion Laboratory,
Edwards, Calif.*

Nomenclature

A	= parameter given by Eq. (6a)
B	= parameter given by Eq. (6b)
C	= parameter given by Eq. (6c)
C_D	= drag coefficient
C_F	= thrust coefficient
D	= plume drag
F	= missile thrust
h	= enthalpy
M	= Mach number
P	= static pressure
q	= dynamic pressure
R	= gas constant
r	= plume radius
ΔS	= entropy change
T	= plume temperature
v	= plume velocity
γ	= ratio of specific heats
ϵ	= expansion ratio
ρ	= plume density
ξ	= parameter given by Eq. (5) or (9)

Subscripts

c	= combustion chamber conditions
e	= nozzle exit plane conditions
I	= plume-freestream interface
max	= maximum value
0	= isentropic
∞	= freestream conditions

I. Introduction

SEVERAL different techniques are available for calculating the gasdynamic properties of low altitude (≤ 60 km) rocket exhausts. Many of the available models^{1,4} assume that the exhaust can be approximated as a constant pressure turbulent reacting shear layer, with the pressure equal to the static pressure of the ambient atmosphere. Physically, this is no doubt a reasonable assumption. In addition, the constraint of constant pressure greatly reduces the mathematical complexity of the model. Shock waves are eliminated, as are imbedded regions of subsonic flow.

However, by making this constant pressure assumption, the model has increased the importance of the initial conditions (temperature, velocity, species concentrations, and physical size). At the same time, it has eliminated a procedure to calculate them. The temperatures, concentrations, and overall size of the plume scale more or less with these initial conditions. Hence, some reliable, global model of the initial expansion region from the nozzle exit pressure to the ambient static pressure must be employed. Unfortunately, none of the models, with one exception, gives any guidance as to how one should calculate these start-line conditions.

In this Note, a simple, easy to employ technique is presented to arrive at appropriate input parameters which are in good agreement with more complicated and complete

calculations. The method, described below, is based on the solution to the global balance equations of mass, linear momentum, and energy. The plume drag which appears in the penultimate balance is calculated by introducing a drag coefficient. Such a method was used by Woodroffe,³ among others. The difference between the models is that in the present method the drag coefficient is calculated on the basis of the drag from the "universal plume" model of Jarvinen and Hill.⁵ This method of determining the drag has certain advantages over the calculation used by Woodroffe, where drag is determined by Newtonian impact pressure.

II. Analysis

Rather than employ the differential forms of the conservation equations in this initial expansion region, which necessitate accounting for two velocity components, shock waves, Mach disks, and imbedded subsonic regions, we can ignore the details of the flow and apply the equations in their integrated form. We assume that the exhaust plume expands from the nozzle exit conditions and at some point not too far downstream reaches the ambient static pressure.

Several balance equations are available. For nonreacting flows, there are the integrated forms of the equations of conservation of mass, energy, linear momentum, and the entropy inequality. They are not all independent; only three of them are required. Common practice in the past has been to use equations of conservation of mass and energy, and to replace the entropy inequality by an equality; i.e., to assume the expansion is isentropic. Such an approach is certainly unrealistic since, as evidenced by the existence of shock waves, the flow is nonisentropic.

Two other approaches may be followed. We could either prescribe some entropy production in the plume or substitute one of the remaining integral conservation equations for the entropy inequality. Woodroffe took the latter approach, using the integral momentum balance. Following his lead, we write the integral balance equations of mass, energy, and linear momentum as⁶:

$$\rho_e v_e r_e^2 = \rho v r^2 \quad (1a)$$

$$h_e + \frac{1}{2} v_e^2 = h + \frac{1}{2} v^2 \quad (1b)$$

$$\rho_e v_e^2 r_e^2 - \rho v^2 r^2 + (P_e - P_\infty) r_e^2 + \int_S (P_I - P_\infty) 2r dr = 0 \quad (1c)$$

In writing these equations we have assumed that entrainment of the freestream into the exhaust plume, turbulent fluctuations, gravitational forces, heat conduction, viscous forces, radiation losses, and work done by expansion are all negligible. By ignoring the equations of species conservation, we have assumed implicitly no chemical reactions occur. All of these assumptions are valid for an expansion region which is small compared to the total plume size.

Introducing a drag coefficient

$$C_D \equiv \frac{I}{\frac{1}{2} \rho_\infty v_\infty^2 \pi r^2} \int_S (P_I - P_\infty) 2\pi r dr \quad (2)$$

we can rewrite the momentum balance, Eq. (1c), as:

$$\rho_e v_e^2 r_e^2 - \rho v^2 r^2 + (P_e - P_\infty) r_e^2 + \frac{1}{2} \rho_\infty v_\infty^2 r^2 C_D = 0 \quad (3)$$

These algebraic equations can be solved for the conditions at the constant pressure location by some algebraic manipulation, provided we make the further assumption of a perfect gas. In this case:

$$v = (I + \xi) v_e \quad (4a)$$

$$T = [I - M_e^2 (\gamma_e - 1) \xi - \frac{1}{2} M_e^2 (\gamma_e - 1) \xi^2] T_e \quad (4b)$$

Received March 11, 1977; revision received Aug. 29, 1977.

Index categories: Jets, Wakes, and Viscid-Inviscid Flow Interactions; LV/M Aerodynamics.

*Currently Assistant Professor, Clarkson College, Department of Chemical Engineering, Potsdam, N.Y.

$$r = \left[\frac{P_e}{P_\infty} \frac{T}{T_e} \frac{v_e}{v} \right]^{1/2} r_e \quad (4c)$$

where

$$\xi = (-B + \sqrt{B^2 + 4AC})/2A \quad (5)$$

and

$$A = \gamma_e M_e^2 + \frac{\gamma-1}{4} M_e^2 \gamma_\infty M_\infty^2 C_D \quad (6a)$$

$$B = \gamma_e M_e^2 + \frac{\gamma_e-1}{2} M_e^2 \gamma_\infty M_\infty^2 C_D - I + \frac{P_\infty}{P_e} \quad (6b)$$

$$C = I - (P_\infty/P_e) + 1/2 \gamma_\infty M_\infty^2 C_D \quad (6c)$$

The drag coefficient C_D is unknown and must be specified in order to calculate v , T , and r . However, before discussing the various methods which could be used, it is interesting to note the relationship between the drag coefficient and the entropy production in the plume. For a perfect gas, the entropy change is given by⁷:

$$\frac{\Delta S}{R} = \ln \left[\left(\frac{T}{T_e} \right)^{\gamma/(\gamma-1)} \frac{P_e}{P_\infty} \right] \quad (7)$$

If a value were available for ΔS , we could use Eqs. (7, 1b, and 1a) to calculate the temperature, velocity, and area, respectively, at the constant pressure location. On substituting these values into Eq. (2), we find an expression for the drag coefficient

$$C_D = \frac{2(I+\xi)}{\gamma_\infty P_\infty M_\infty^2} \left(\frac{P_\infty}{P_e} \right)^{1/\gamma} e^{-\Delta S(\gamma-1)/\gamma R} [\gamma P_e M_e^2 \xi - P_e + P_\infty] \quad (8)$$

The parameter ξ is now expressed in terms of the entropy change:

$$\xi = -I + \left[I + \frac{2 \left[I - e^{\Delta S(\gamma-1)/\gamma R} \left(\frac{P_\infty}{P_e} \right)^{(\gamma-1)/\gamma} \right]}{M_e^2 (\gamma-1)} \right]^{1/2} \quad (9)$$

As the entropy change decreases, ξ and the drag coefficient both increase. Since the entropy change is nonnegative, the maximum value of C_D occurs for an isentropic expansion. Equations (4-6), with Eqs. (8) and (9), and $\Delta S=0$ are completely equivalent to the more common expression for isentropic expansions, as may be found, for example, in Sutton.⁸ The lower bound on C_D , corresponding to the smallest possible value of ξ , is 0. This is the case of a quiescent freestream.

In order to apply Eqs. (4-6) to calculate the start-line conditions, an expression for the drag coefficient, or alternatively the entropy production, in the near field is required. An accurate prescription of this coefficient would involve a detailed calculation of the plume expansion, so that the plume interface pressure as a function of distance, and hence the integral in Eq. (2), can be evaluated. This is just the kind of detail which we hoped to avoid by using the integral approach in the first place. Woodroffe eschews this difficulty by assuming a source flow model for the plume expansion with a Newtonian impact pressure for the freestream. This approach involves additional computer calculations to evaluate C_D . While this is certainly much less effort than would be involved in a complete calculation of the expansion region, it does detract somewhat from the simplicity of the integral balance approach.

Boynton⁹ has reported a much simpler method for evaluating C_D . Assuming a parabolic shape for the plume interface and Newtonian impact pressure, he arrives at the following expression for the drag coefficient:

$$C_D = (2/M_\infty^2) \ln(I + M_\infty^2) \quad (10)$$

However, both of these approaches might be expected to overpredict the actual drag coefficient, since both take no account of the actual entropy production (i.e., the complex shock structure) within the expansion region.[†]

Several years ago, Jarvinen and Hill⁵ brought together the many scaling laws which had been developed up to that time for the initial size and shape of the near-field rocket plume. These scaling laws were shown to be in agreement with experimental observations of the exhausts of missiles in flight. Jarvinen and Hill predicted that all exhaust plumes could be collapsed into a "universal plume shape," with the radial and axial distances appropriately scaled.

If we define C_D in terms of the plume drag as

$$C_D = D/q_\infty A_{\max} \quad (11)$$

and note that according to the universal shape of plumes the maximum interface radius is $0.75 [(FD)^{1/2}/q_\infty]^{1/2}$, we can write

$$C_D = 16/9\pi (D/F)^{1/2} \quad (12)$$

Furthermore, according to Jarvinen and Hill, the thrust-to-drag ratio of a given missile is a constant given by

$$D/F = (C_{F\max}/C_F) - I \quad (13)$$

where

$$C_{F\max} = \left[\frac{2\gamma^2}{\gamma-1} \left(\frac{2}{\gamma+1} \right)^{\frac{\gamma+1}{\gamma-1}} \right]^{1/2}$$

and

$$C_F = C_{F\max} \left[I - \left(\frac{P_e}{P_c} \right)^{\frac{\gamma-1}{\gamma}} \right]^{1/2} + \frac{P_e - P_\infty}{P_c} \epsilon \quad (14)$$

While the scaling of the universal plume may be expected to be valid only at relatively high altitudes, it should be recalled that, as mentioned by Woodroffe, the predictions of Eqs. (3-5) are relatively insensitive to C_D at low altitude since the vehicle Mach numbers are low and the freestream pressure high.

III. Results

Start-line properties of constant pressure low altitude plumes were predicted using the different models for C_D just discussed. The calculations were based on the selection of exit plane and trajectory parameters given in Table 1 for case A. These were chosen since other calculations, using a more complete model for the initial expansion region, were available for comparison. The method of Woodroffe was also compared to the present method by using the missile and trajectory parameters (case B of Table 1) for which he calculated start-line properties.

The amount of entropy produced in the near-field expansion for both cases, using three expansion methods, is given in Figs. 1 and 2. Shown in the figures is the case of zero drag, the upper bound on the amount of production, and isentropic expansion, the lower bound. For the case A

[†]Boynton proposed this equation several years ago and acknowledges its inadequacy.

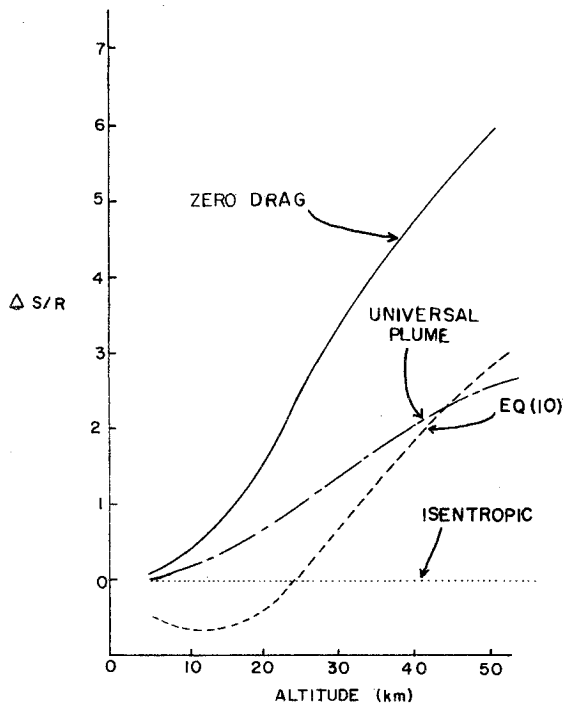


Fig. 1 Entropy production in initial expansion region for case A missile parameters.

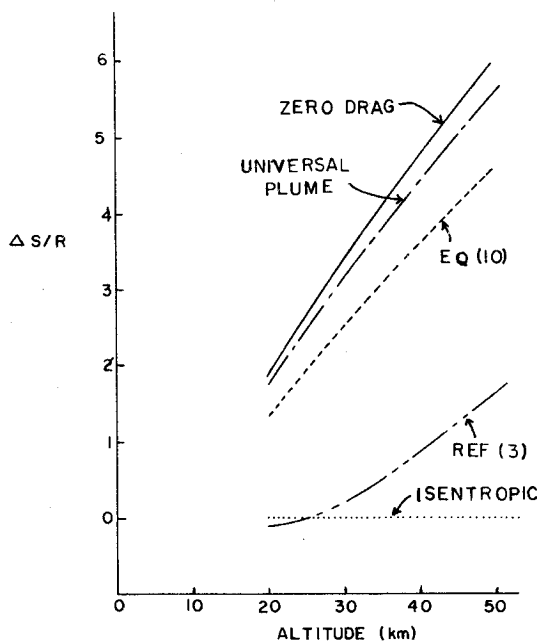


Fig. 2 Entropy production in initial expansion region for case B missile parameters.

parameters, Eq. (10) gives a negative entropy production at low altitudes: it violates the second law of thermodynamics. Likewise, Woodroffe's method, in case B, also gives an entropy decrease at low altitude. Another interesting feature of Fig. 2 is that the entropy production based on Woodroffe's model for C_D is significantly below those using Eq. (10) and the universal plume model for C_D . The latter two are much closer to the zero drag, maximum entropy production limit. This result is not unexpected, since the vehicle Mach numbers used in Woodroffe's example are quite low as compared to those used in case A, which is more representative of a missile in flight.

In order to be consistent with a positive entropy production in the near field, the plume drag coefficient must be less than

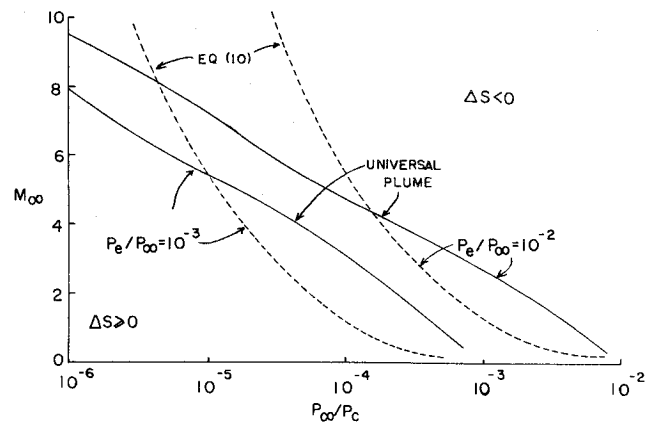


Fig. 3 Allowable Mach number range for drag to satisfy the entropy inequality: —, universal plume drag; ---, Eq. (10).

the isentropic drag coefficient. To facilitate a direct comparison between the drag coefficient deduced from the universal plume model, Eqs. (12-14), and isentropic drag coefficient, Eqs. (8) and (9) with $\Delta S=0$, we can assume the nozzle expansion from chamber conditions to exit conditions is isentropic.⁸ In this case, both C_D and $\gamma_\infty M_\infty^2 C_{D0}$ are functions only of the pressure ratios P_∞/P_c , P_e/P_c and the ratio of specific heats, γ . For given values of P_e/P_c and γ , the variation of these two drag coefficients with P_∞/P_c can be interpreted as giving the allowable vehicle Mach number range, at each altitude, for which the universal plume drag coefficient satisfies the second law of thermodynamics. This Mach number range is shown in Fig. 3, which includes values of γ from 1.2 to 1.3. For a given value of P_e/P_c , any Mach number below and to the left of the curve will result in $C_D < C_{D0}$. On the other hand, for Mach numbers above and to the right of the curve, $C_D > C_{D0}$, and the second law will be violated. It can be seen from this figure that the allowable Mach number increases with altitude and is representative of vehicle velocities encountered in practice. Also shown on the figure is the allowable upper bound on the Mach number necessary for Eq. (10) to satisfy the entropy inequality. As can be seen, at low altitudes the allowable vehicle Mach number is less than that needed by the universal plume drag. This is the reason for the negative entropy production predicted by Eq. (10) for case A (Fig. 1).

The predictions of the various models for plume temperature and radius ratio at the matched pressure point is illustrated in Fig. 4. The assumption of no drag gives the upper bound on temperature and radius. An isentropic expansion should give the lower bound. However, at low altitudes and Mach numbers, Eq. (10) violates the second law, and so this technique gives temperatures less than the isentropic expansion. The predictions using the drag coefficient given by Eq. (12) falls between the two extremes. Also shown

Table 1 Exit plane and trajectory parameters

Case A: $\gamma_e = 1.23$; $P_e = 13.6$ psia; $T_e = 1850K$; $P_c = 790$ psia; $M_e = 3.06$; $\epsilon = 8$		
Alt, km	P_∞ , psi	M_∞
5	7.8	0.7
25	0.365	2.8
35	0.083	3.7
50	0.0116	4.9
Case B: $\gamma_e = 1.25$; $P_e = 14.7$ psia; $T_e = 2000K$; $P_c = 515$ psia; $M_e = 2.88$; $\epsilon = 5$		
Alt, km	P_∞ , psia	M_∞
20	0.8	0.7
30	0.17	1.0
50	0.0116	1.4

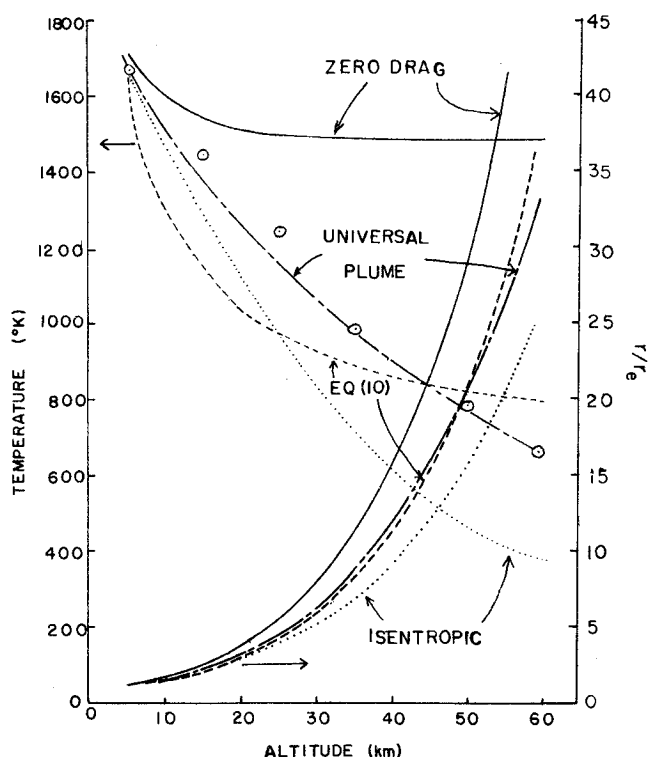


Fig. 4 Prediction of temperature and radius ratio at matched pressure location: \cdots , isentropic expansion; $—$, zero drag; $—$, universal plume drag; $---$, Eq. (10); \odot Wilson's predictions.

in the figure are temperature predictions reported by Wilson¹⁰ using a more complete, though still approximate, method for calculating the expansion region. That method includes the plume shock, Mach disk, and reflected shock, although approximately. That the technique described here, using a drag coefficient based on the universal plume shape, is in excellent agreement with the more complex model indicates that the present model for C_D does account for the entropy production within the expansion region.

IV. Conclusions

A mathematical model for a low altitude plume which assumes that the plume is at constant pressure is limited, to a large extent, by the accuracy of the input conditions for the model: the temperature, concentrations, velocity, and size of the plume at the matched pressure point. Integral balances of mass, momentum, and energy can be employed to solve for these input conditions. A method of prescribing a drag coefficient has been identified which has three favorable attributes: it is extremely easy to employ; it is in agreement with the second law of thermodynamics; and it gives answers which agree with more complete calculations of the expansion.

References

- ¹Pergament, H. S. and Calcote, H. F., "Thermal and Chemionization Processes in Afterburning Rocket Exhausts," *Eleventh Symposium (International) on Combustion*, The Combustion Institution, Pittsburgh, 1967, pp. 597-611.
- ²Mikatarian, R. R., Kau, C. J. and Pergament, H. S., "A Fast Computer Program for Nonequilibrium Rocket Plume Predictions," Air Force Rocket Propulsion Laboratory Technical Report AFRPL-TR-72-94, 1974.
- ³Woodroffe, J. A., "One Dimensional Model for Low Altitude Rocket Exhaust Plumes," AIAA Paper 75-224, Pasadena, Calif., 1975.
- ⁴Jensen, D. E. and Wilson, A. S., "Prediction of Rocket Exhaust Flame Properties," *Combustion and Flame*, Vol. 25, 1975, pp. 43-55.

⁵Jarvinen, P. O. and Hill, J. A. F., "Universal Model for Underexpanded Rocket Plumes in Hypersonic Flow," presented at 12th JANNAF Liquid Propulsion Meeting, Las Vegas, 1970.

⁶Slattery, J. C., *Momentum, Energy and Mass Transfer in Continua*, Wiley, New York, 1972, Chaps. 4 and 7.

⁷Liepmann, H. W. and Roshko, A., *Elements of Gasdynamics*, Wiley, New York, 1957, p. 20.

⁸Sutton, G. P., *Rocket Propulsion Elements*, Wiley, New York, 1964, pp. 40-41.

⁹Boynton, F. P., Personal communication, Physical Dynamics, Inc., May 1976.

¹⁰Wilson, K. H., "Discussion of the AFRPL Evaluation of the LMSC-PARL Low Altitude Flowfield Model," Lockheed Missiles and Space Company, Inc., Palo Alto Research Labs Rept. LMSC-D012442, 1976.

Correlation of Turbulent Shear Layer Attachment Peak Heating Near Mach 6

J. Wayne Keyes*

NASA Langley Research Center, Hampton, Va.

Nomenclature

- BS, IS, SL = curved bow shock, plane impinging shock, shear layer, Fig. 1
- c_p = specific heat at constant pressure
- d = body diameter
- h = heat-transfer coefficient
- M = Mach number
- p = static pressure
- T = temperature
- u = velocity
- X_{SL} = total length of shear layer, Fig. 1
- $\delta_{SL,T}$ = turbulent shear layer thickness at attachment
- θ_{SL} = shear layer angle relative to local inclination
- μ = viscosity
- ρ = density, ($\rho_w \propto p_p / T_w$)

Subscripts

- 1, 2, 3, 4, 5 = regions in flowfield, Fig. 1
- local = local value upstream of separation
- p = peak
- w, ∞ = wall and freestream, respectively

Introduction

KNOWLEDGE of peak heating in regions of interfering flows, in particular shear layer attachment, is important in the design of components of high-speed vehicles, such as inlet cowl lips, wing and fin leading edges and surface panels, and external protuberances. Investigations of two- and three-dimensional attachment heating were reported in Refs. 1-5. A correlation of free shear layer attachment peak heating on hemispheres was made in Ref. 6.

This Note presents a correlation of new turbulent two-dimensional data and peak heating data for attaching free shear layers from Refs. 3 and 7. The present data were obtained on a 2.54-cm and 5.08-cm-diam cylindrical leading-edge slab 25.4-cm long with widths of 7.62 cm and 10.16 cm, respectively. A sharp leading-edge flat plate (30.48-cm long by 25.4-cm wide) set at 15 and 20 deg was used to generate plane

Received April 25, 1977; revision received July 18, 1977.

Index categories: Boundary Layers and Convective Heat Transfer—Turbulent; Jets, Wakes, and Viscid-Inviscid Flow Interactions; Supersonic and Hypersonic Flow.

*Aerospace Engineer, Fluid Mechanics Branch, High-Speed Aerodynamics Division.